Journal of Volcanology and Geothermal Research 450 (2024) 108067

Contents lists available at ScienceDirect

Journal of Volcanology and Geothermal Research

journal homepage: www.journals.elsevier.com/journal-of-volcanology-and-geothermal-research

An air-fall ash layer in the Grotta dei Baffoni cave in the Frasassi Gorge (Marche Apennine, Italy): Relevance to the Younger Dryas debate

Alessandro Montanari [a], Christian Koeberl [b,*], Toni Schulz [b], Victoria C. Smith [c], Mihály Molnár [d], Katalin Tóth-Hubay [d]

[a] Osservatorio Geologico di Coldigioco, Cda. Coldigioco 4, 62021 Apiro, Italy
[b] Department of Lithospheric Research, University of Vienna, Josef-Holaubek-Platz 2, A-1090 Vienna, Austria
[c] University of Oxford, Research Laboratory for Archaeology and the History of Art, South Parks Road, Oxford OX1, UK
[d] Atomki Institute for Nuclear Research, Bem tér 18/c, Debrecen 4026, Hungary

ARTICLE INFO

Keywords:
Northern Apennines
Frasassi caves
Upper Pleistocene tephra
Younger Dryas
Older Dryas
Climate change

ABSTRACT

A thin tephra layer was discovered in a section of cave sediments in the Grotta dei Baffoni Cave (GDB), in the Marche Apennine of central Italy, immediately underlying a clayey layer containing charcoal fragments dated at 12,843 ± 122 years before present. This date indicated that humans were occupying the cave at the very beginning of the Younger Dryas cooling event. Petrographic and geochemical analysis of the volcanic glass contained in the tephra layer suggests that this deposit represents a distal air-fall ash erupted from a volcano in the Campi Flegrei caldera, which produced the Neapolitan Yellow Tuff (NYT). Radiocarbon AMS dating of charcoal particles from this GDB tephra layer yielded an age around 14.4 ± 0.4 ka, which is consistent with the chronology of the NYT eruption, which occurred some 14.1 ± 1.4 thousand years ago. Nevertheless, the sediment succession in this cave deposit actually covers a time interval across the sudden and drastic Younger Dryas cooling event, which occurred around 12.9 ka. There is an ongoing debate about the causes of the Younger Dryas event, which divides the scientific community into a faction sustaining that the Younger Dryas cooling event was triggered by an elusive meteorite impact, and an opposing one that advocates volcanic eruptions, such as the eruption of the Laacher See volcano in central Germany, which was precisely dated at 13 ka. A detailed trace element and $^{187}Os/^{188}Os$ analysis of the sedimentary succession in the Grotta dei Baffoni Cave did not reveal evidence of any platinum-group element anomalies or an osmium isotope signature that would support an extraterrestrial impact event around the time of the Younger Dryas event. The Grotta dei Baffoni tephra layer turned out to be derived from a large eruption in the Campi Flegrei of southern Italy, which produced the huge Neapolitan Yellow Tuff around 14.1 thousand years ago. This catastrophic event appears to be synchronous with the minor Older Dryas cooling event, which preceded the Younger Dryas by some 1300 years.

1. Introduction

During an interdisciplinary study of the upper Pleistocene-Holocene sedimentary succession in the shallow Grotta dei Baffoni Cave (Frasassi Gorge, Marche region of central Italy; 43°24′05" N; 57°50′25″ E; 270 m asl), Montanari et al. (2022a) dug a small pit and drilled a ~ 80-cm-deep auger core (PIT-2/H-2) at the far northern end of the cave, some 40 m from the wide, south facing entrance (Fig. 1A). A ~ 10-cm-thick speleothemic crust (Fig. 1B) was sealing a stratified deposit of silty lime containing terrestrial gastropod shells, small animal bones (lizards, bats, rodents), and limestone clasts (Fig. 1C). Layer 2 immediately underlying the speleothemic crust contained also charcoal particles, which have been ^{14}C AMS dated at 12965–12721 cal yr BP (2σ), i.e., 12,843 ± 122 yr BP. This deposit was interpreted by Montanari et al. (2022a) as cave soil that was washed out by the runoff from the atrial area of the cave, eventually settling down into a now-dry water pool. The charcoal was interpreted as deriving from fires lit by early occupants in the atrial area of the cave, suggesting that the cavern was frequented by hunter-gatherer people during the Younger Dryas cold period.

Originally, Montanari and coworkers noticed a bright orange-

* Corresponding author.
E-mail addresses: christian.koeberl@univie.ac.at (C. Koeberl), toni.schulz@univie.ac.at (T. Schulz), victoria.smith@arch.ox.ac.uk (V.C. Smith), mmol@atomki.hu (M. Molnár), hubaykatalin@isotoptech.hu (K. Tóth-Hubay).

https://doi.org/10.1016/j.jvolgeores.2024.108067
Received 3 January 2024; Received in revised form 27 March 2024; Accepted 30 March 2024
Available online 3 April 2024
0377-0273/© 2024 The Authors. Published by Elsevier B.V. This is an open access article under the CC BY-NC-ND license (http://creativecommons.org/licenses/by-nc-nd/4.0/).

colored, ~1–2 cm-thick horizon at the base of the charcoal-bearing Layer 2, but thought that it represented a normal oxidation band. After re-sampling the six layers exposed in PIT-2, we found that the thin orange Layer 3 was essentially comprised of tephra. Actually, the fine sand-size fraction making up 16 wt% of the bulk sediment is entirely made up of volcanic glass shards and lapilli (Fig. 2). This discovery led us to investigate the alternative hypothesis that Layer 3 represented an air fall volcanic ash produced by the Laacher See volcano in central Germany at 13.006 ± 9 yr BP (e.g., Reinig et al., 2021, and references therein).

For >15 years now, there has been an intense controversy in the Earth science community about the causes of the Younger Dryas cooling event. This climatic event suddenly occurred ~12,900 years ago lasting to ~11,700 years ago, i.e. to the beginning of the Holocene warm period in the northern hemisphere. The sudden freezing occurred in a matter of a few decades when, in the northern hemisphere, atmospheric temperatures were on the rise reaching an environmental condition similar to a post-glacial climatic regime. A common hypothesis used to explain the cooling event is related to catastrophic meltwater drainage from glacial Lake Agassiz as a trigger for large-scale ocean circulation change (e.g., Norris et al., 2021, and references therein). This cooling initiated more or less an instant glaciation, causing the extinction of the upper Pleistocene megafauna and a bottleneck in the evolutionary expansion of *Homo sapiens*.

The controversy was ignited mainly by Firestone et al. (2007), who alleged that the primary trigger for the Younger Dryas cooling event was an elusive meteorite impact, or a comet, or an airburst, all surprisingly leaving no crater behind, either of which supposedly caused an immediate alteration of the global climate. This hypothesis was criticized in the following years by many geologists (e.g., Paquay et al., 2009; Pinter et al., 2011; Sun et al., 2020, 2021, and references therein), as the proposed evidence for impact was not in agreement with known impact physics or impact signatures, and who supported instead an episodic and volcanic origin to explain the observed geochemical anomalies, such as at the Hall's Cave (Sun et al., 2020) and Friedkin (Sun et al., 2021) sites, Texas, as the cause of the Younger Dryas climate event. Recently, Holliday et al. (2023) provided a comprehensive discussion of all the problems and inconsistencies related to the Younger Dryas impact hypothesis.

Reinig et al. (2021) synchronized the Younger Dryas cooling event with the explosion of the Laacher See volcano in central Germany, finding abundant burned-tree remains dated at 13,006 yr BP, which were associated with volcanic ejecta in a number of lacustrine deposits throughout northern European and southern Alpine regions. The burned trees were attributed to immense forest fires, which were ignited by the eruption of the Laacher See volcano. Sun et al. (2020) also proposed that the ~150-years-delay of the Younger Dryas event, which occurred ~12,850 years ago, in respect to the Laacher See eruption, was due to the fact that the forest fires produced an enormous amount of CO_2, which, associated with the volcanic degassing, triggered a greenhouse effect.

The rapidly increasing temperature of the Earth's surface would have accelerated the melting of Arctic ices, which eventually would have caused a collapse of the thermohaline circulation in the North Atlantic

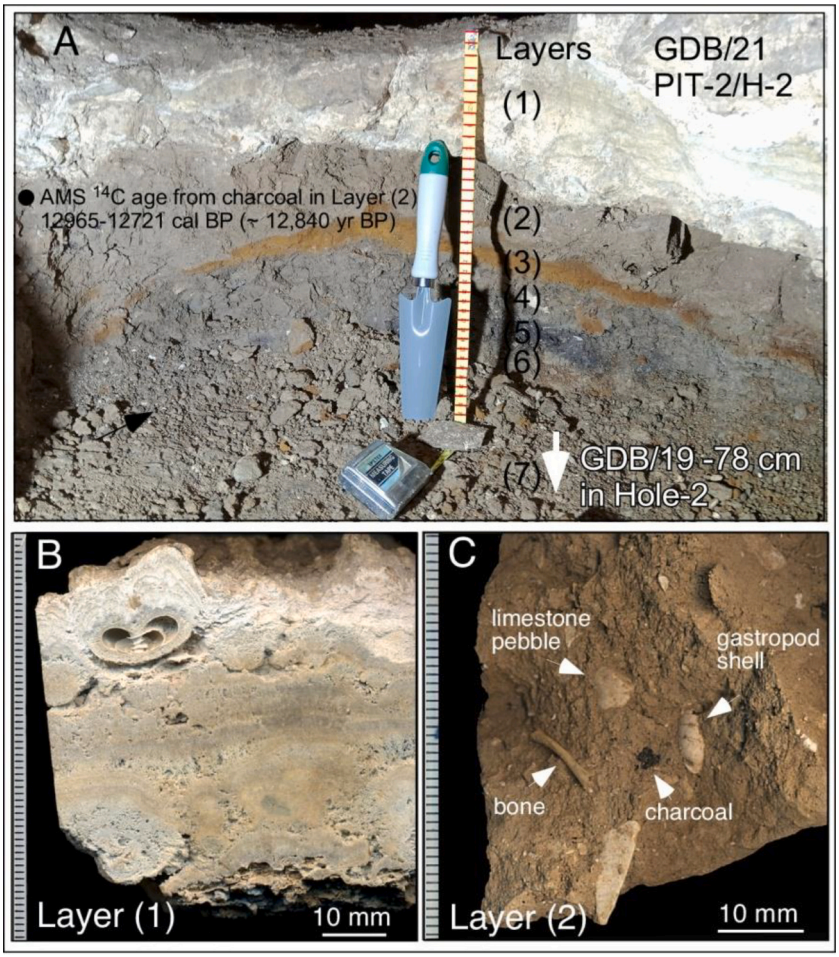

Fig. 1. A) Partitioning of layers of the sedimentary succession exposed in PIT-2 in the Grotta dei Baffoni Cave; B) Close up photograph of calcite crust of Layer 1; C) Close up photograph of a section of Layer 2.

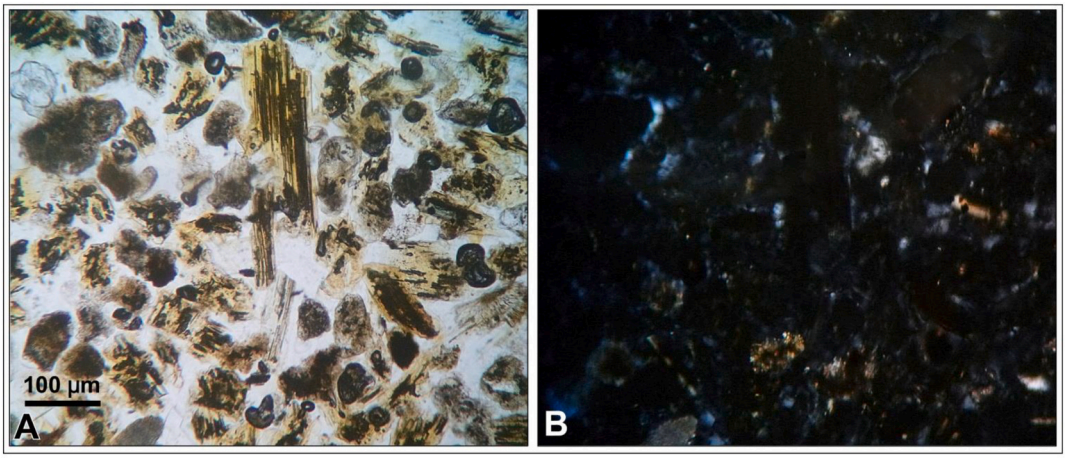

Fig. 2. A) Transmitted plain light microphotograph of a > 62 µm grain mount thin section of the tephra from Layer 3; B) The same frame under crossed polarizers.

Ocean, with consequent immediate freezing of the northern hemisphere land masses. This hypothetical scenario is nevertheless worrying inasmuch it somewhat reflects the present climate change phenomenon, with the difference that in the Late Pleistocene the trigger for the Younger Dryas freezing event was a natural yet exceptional phenomenon, such as the explosion of a volcano, whereas for the present global warming situation, the trigger was a non-natural yet exceptional human phenomenon, i.e., the Industrial Revolution.

In this work, we performed a detailed integrated stratigraphic analysis (mineralogy and petrography, trace element geochemistry, osmium isotopes, accelerator mass spectrometry (AMS), radiocarbon geochronology) of the sedimentary succession in the Grotta dei Baffoni Cave across the Younger Dryas interval to check for the possible presence of an extraterrestrial component attributable to a hypothetical meteorite impact, which revealed the actual provenance of the tephra layer, and the age frame of this interval.

2. Samples, methods, and techniques

The six layers shown in Fig. 1A were sampled using a trowel on September 26, 2021, and collected in labelled zip-lock bags. Sample from layer 7 was already available from Core H-2 auger-drilled in 2019 by Montanari et al. (2022a). About 100 g of each dry sample was wet-washed using a 63 µm polyester filter, and the dry residues were sieved with a stack of standard sieves to determine the grain size distribution. Calcium carbonate content was determined using a Dietrich-Früling water calcimeter (precision ±2 wt%) and calibrated with a Carrara marble standard. Total organic carbon content (C_{org}) was determined by the loss on ignition method (LOI).

Aliquots of the seven samples were analyzed at Vienna for trace elements using methods and techniques described by Mader and Koeberl (2009), and for selected highly siderophile element abundances and Re-Os isotope ratios as described by Schulz et al. (2017) and references therein.

For highly siderophile elements (HSE) and Re-Os isotope studies, about 0.5 g of homogeneous powder of each sample was spiked with a mixed tracer composed of ^{185}Re, ^{190}Os, ^{191}Ir, and ^{194}Pt, ^{99}Ru, and ^{105}Pd isotopes and digested in 6 mL inverse aqua regia at 250 °C and 100–130 bar in an Anton-Paar high pressure asher for 4 h. Digestion and Os and HSE separation was performed using techniques described in Cohen and Waters (1996), Pearson and Woodland (2000), Luguet et al. (2008, 2015)), and summarized in Schulz et al. (2016). The remaining aqua regia fraction and the undissolved sample was dried down, re-dissolved with HF, and finally processed over anion columns (AG 1-X8, 100–200 mesh; Rehkämper and Halliday, 1997). All chemical processing was performed in Vienna, HSE measurements carried out using a single collector Element XR instrument at the Freie Universität Berlin, and Os isotope measurements conducted on a Triton TIMS XT at the Department of Lithospheric Research in Vienna. Reproducibility of DROsS (Durham Romil Osmium Standard) solution, for loads between 10 and 100 pg, is 0.16086 ± 0.00075 (n = 3), which is in agreement with previously reported values (0.160924 ± 0.000004, Luguet et al., 2008). The Os total procedural blank was <1 pg (n = 2), mostly contributing <5 rel% to the measured Os concentration of all samples. All Os isotope data were corrected for blank contributions.

Highly siderophile elements were measured using a Thermo Element XR SF-ICP-MS in single collector mode at the Freie Universität Berlin, Germany, using methods and interference corrections as described in Luguet et al. (2015). Total blanks for this study (n = 2) were 5 pg for Re, 1 pg for Ir, ~43 pg for Pt, 34 pg for Ru and 61 pg for Pd. All reported concentration values are blank-corrected.

A Jeol JXA-8200 wavelength-dispersive electron microprobe in the

Table 1
Grain size, calcium carbonate, and total organic carbon analyses of the sedimentary sequence in PIT-2/H-2 from the Grotta dei Baffoni Cave.

Layer (n.) and site	Sediment	Depth (cm)	$CaCO_3$ (wt%)	Corg (wt%)	<63 mm (wt%)	63–2000 mm (wt%)	>2000 mm (wt%)
(1) GDB/21 Pit-2	calcite crust	0–10	~100	~0	//	//	//
(2) GDB/21 Pit-2	silty lime bulk	14 ± 4	36.84 ± 2	5.84	80.80	14.60	4.60
(3) GDB/21 Pit-2	tephra bulk	20 ± 1	12.94 ± 2	19.84	83.80	16.00	0.20
(3)* GDB/21 Pit-2	tephra <63 mm	20 ± 1	10.91 ± 2	14.66	89.00	10.30	0.70
(3)* GDB/21 Pit-2	tephra 250–500 mm	20 ± 1	//	19.48	89.00	16.00	0.20
(4) GDB/21 Pit-2	silty lime bulk	22 ± 2	22.80 ± 2	5.98	93.30	5.00	1.70
(5) GDB/21 Pit-2	silty lime bulk	27 ± 2	38.96 ± 2	4.46	74.20	12.80	13.00
(6) GDB/21 Pit-2	silty lime bulk	32 ± 2	40.81 ± 2	3.81	70.80	15.00	14.20
(7) GDB/19H-2	silty lime bulk	78 ± 8	42.28 ± 2	2.87	52.10	18.10	29.80

Note: All grain size analyses were done on 200 g dry bulk sediment; * = second run from same sample.

Table 2
Trace and minor element abundances of the sedimentary succession of the Grotta dei Baffoni Cave.

Layer (n.) and site	(1) GDB/21-Pit2	(2) GDB/21-Pit2	(3A) GDB/21-Pit2	(3B) GDB/21-Pit2	(4) GDB/21-Pit2	(5) GDB/21-Pit2	(6) GDB/21-Pit2	(7) GDB/19-H2
Na (wt%)	102*	0.39	0.71	0.79	0.59	0.47	0.45	0.39
K (wt%)	24.3*	1.20	1.74	1.9	1.75	1.01	1.10	0.91
Sc	0.09	7.02	6.43	6.18	10.8	7.20	6.86	5.75
Cr	5.64	56.4	17.9	20.7	89.8	59	61.3	53.2
Fe (wt%)	305*	2.40	4.79	3.92	3.16	2.09	1.92	1.6
Co	0.23	13.3	8.07	35.9	20	11.8	11	9.15
Ni	<4	51	35.1	47	68	64	48	42
Zn	14	249	172	358	360	230	163	103
Ga	<0.5	3.5	8.4	5.1	7.1	5.0	2.6	3.6
As	3.22	6.95	19	13.2	8.47	4.99	4.76	4.33
Se	<0.5	11.3	1.1	<1.9	<1.9	<1.5	<1.6	<1.5
Br	8.3	15	32	28	15	15	9.9	4.3
Rb	0.81	82.9	83.1	106	114	73.9	69.3	59.7
Sr	33	85	140	104	94	103	105	98
Zr	<2	241	648	546	262	178	150	139
Sb	0.30	0.47	0.45	0.63	0.63	0.35	0.36	0.30
Cs	0.14	10.2	6.45	7.29	9.77	4.93	4.27	3.67
Ba	14	205	1097	1733	235	175	147	137
La	0.27	35.9	114	115	34.8	24.3	22.1	19.0
Ce	0.39	61.8	206	337	59.4	42.4	38.1	32.6
Nd	<0.6	27.5	80.2	81.3	28.2	18.5	16	14.6
Sm	0.02	6.15	14.7	14.4	6.71	4.48	4.28	3.75
Eu	0.03	1.20	3.40	3.14	1.28	0.89	0.81	0.69
Gd	<0.1	4.69	12.8	11.2	5.22	3.73	3.68	3.53
Tb	<0.01	0.81	1.77	1.71	0.95	0.64	0.58	0.53
Tm	0.23	0.39	0.76	0.63	0.39	0.29	0.32	0.29
Yb	0.01	2.26	4.76	4.14	2.89	1.87	1.79	1.53
Lu	0.01	0.34	0.71	0.62	0.43	0.28	0.26	0.23
Hf	0.05	4.18	11.0	8.70	4.72	3.15	2.85	2.60
Ta	<0.01	1.23	4.42	3.23	1.03	0.75	0.65	0.58
Ir (ppb)	<0.4	<1.5	<2.1	<1.6	<1.8	<1.5	<1.5	<1.5
Au (ppb)	<1	0.8	1.07	1.2	0.7	<2	<2	<2
Th	0.08	13.6	55.0	33.8	10.9	7.74	7.12	6.16
U	<0.04	1.88	2.5	<1.3	2.9	1.86	1.82	1.81

Note: Data by INAA, in ppm except as noted. *ppm.

School of Archaeology, University of Oxford, was used to take back-scattered electron images and determine the tephra glass compositions. The analyses of the glass shards were conducted at 15 kV using 6 nA current and 10-μm beam. This relatively low current and the defocused beam were selected to minimize Na loss. The instrument was calibrated using a range of mineral standards, and the calibration was checked by analyzing reference glasses from the Max Planck Institute (MPI-DING glasses; Jochum et al., 2006). The following elements were analyzed: Si, Al, Na, Mg, Cl, P, Ti, K, Ca, Mn, and Fe. Count times were 30 s on peak and background counts were collected for half that time on either side of the peak for all elements except Na (12 s on peak) and Cl, P, Mg, and Mn (50 s). All data were normalized to 100% for comparative purposes, and the raw data and secondary standard analyses are included in Table X in the Supplementary Material.

The organic carbon components in bulk sediment from Layer 2 (sample GDB/21-PIT2-L2) and Layer 3 (sample GDB/21-PIT2-L3), as well as discrete charcoal particles (sample GDB/21-PIT2-L3-charcoal) and gastropod shell fragments (sample GDB/21-PIT2-L3-shell), were ^{14}C-dated by the EnvironMICADAS AMS equipment at the Hertelendi Laboratory in Debrecen, Hungary, following methods and techniques of Molnár et al. (2013). Bulk sediment samples were demineralized with HCl 1 M at 70 °C (Hatté et al., 2010) and were combusted at a low temperature with the two-step method ("LT" 400 °C), and eventually at a high temperature ("HT" 800 °C) in the presence of oxygen gas in a quartz tube (Jull and Burr, 2006). The charcoal sample was prepared according to a standard protocol using the acid-base-acid (ABA) method with sealed-tube MnO_2 combustion. Shell fragments were treated with standard acid pre-leaching and acid pre-treatment to release CO_2 in a vacuum cell. The resulting CO_2 gas was sealed in a graphitized tube for the ^{14}C AMS measurements. Conventional radiocarbon ages of samples are presented in radiocarbon years before present (BP), where BP refers to 1950 CE (Stuiver and Polach, 1977). All radiocarbon dates were calibrated using the IntCal20 calibration dataset (Reimer et al., 2020).

3. Results and discussion

3.1. Sedimentology

As shown in Table 1, the orange tephra Layer 3 contains ~13 wt% $CaCO_3$, compared to ~23–42 wt% in the other samples from the same section. Even more distinctly, its content of organic carbon of ~15–20 wt% is about 3 to 6 times higher than the other samples. This suggests that the high C_{org} may be attributed to very fine soot particles. However, it cannot be excluded that some carbonate and charcoal particles in this sample came from the overlying Layer 2, therefore representing some contamination during sampling this thin layer with a trowel. In any case it is noteworthy to point out that similar orange bands are present in alluvial Middle Pleistocene slack water deposits in the Grotta della Beata Vergine Cave at Frasassi, and in those cases the bright orange color is due to the presence of oxidized vegetal remains (Pignocchi and Montanari, 2016). Also to be noticed is the fact that the tephra Layer 3 is mostly made of <63 μm particles (84–89 wt%), i.e., silt and clay, with only 10–16 wt% of sand-size grains, and, unlike the other overlying and underlying layers, practically lacks coarser grains (i.e., pebbles or bones). In contrast, Layers 2 and 4 contain a > 2 mm fraction of 4.6 and 1.7 wt%, respectively (see Table 1).

3.2. Chemostratigraphy

In terms of major and trace element data (Table 2), there is no evidence for an extraterrestrial component (along the lines of evidence reviewed in, for example, Koeberl et al., 2012) in any of the seven

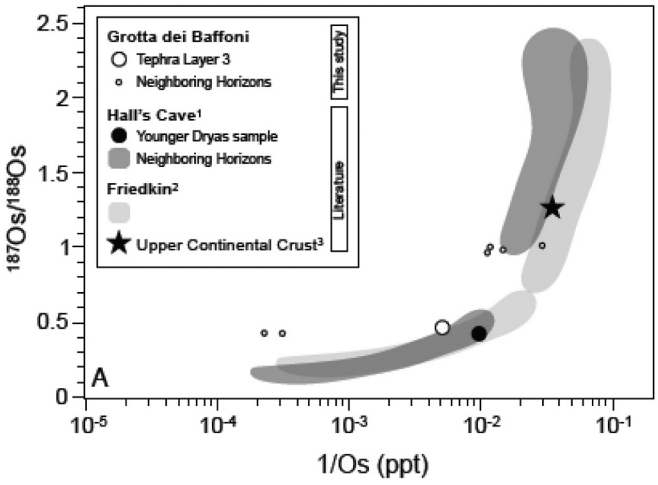

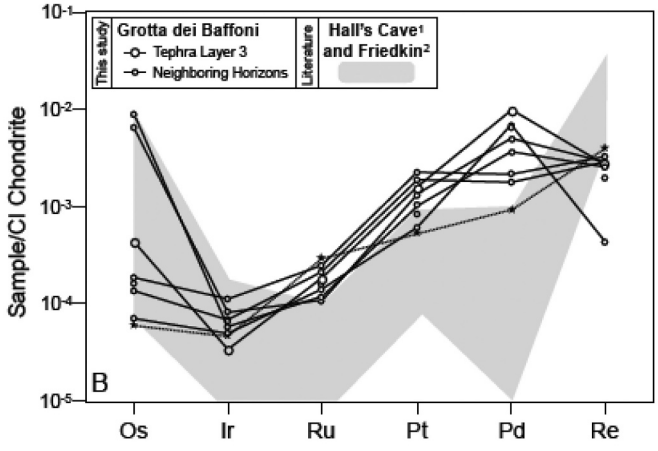

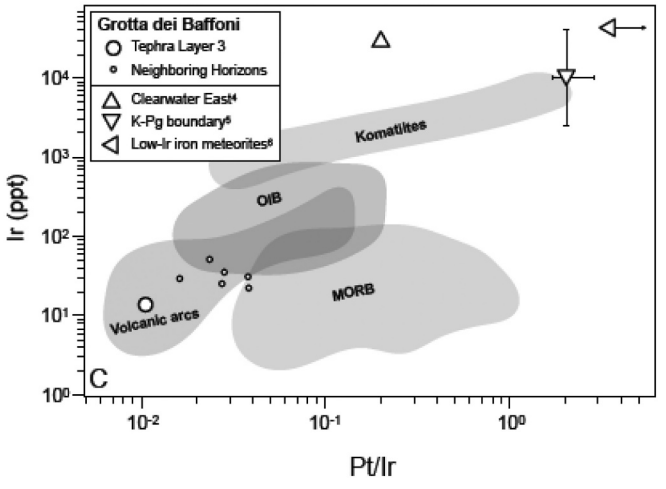

(caption on next column)

Fig. 3. A) $^{187}Os/^{188}Os$ versus 1/Os (ppt) for tephra layer 3 from Grotta dei Baffoni and adjacent strata and, for comparison, literature data for younger Dryas related Hall's Cave sediments and from the Friedkin sampling site. 1 = Sun et al. (2020), 2 = Sun et al. (2021), 3 = Peucker-Ehrenbrink and Jahn (2001). Note that data from Paquay et al. (2009) for sections from Howard Bay, Blackwater Draw, Murray Springs, Lubbock Lake, Topper, and Lommel overlap with the ranges shown for the most radiogenic samples from the three sites shown in the diagram. B) Chondrite-normalized highly siderophile element patterns for tephra layer 3 from Grotta dei Baffoni and adjacent strata. Literature data for Younger Dryas-related Hall's Cave sediments and from the Friedkin sampling site are shown for comparison. 1 = Sun et al. (2020), 2 = Sun et al. (2021). Chondrite values from Anders and Grevesse (1989). C) Iridium vs. Pt/Ir plot showing data for tephra layer 3 from Grotta dei Baffoni and adjacent strata. Ranges for komatiites, volcanic arc rocks, mid-ocean ridge basalts, and oceanic island basalts are shown for comparison (see Sun et al., 2020, and references therein). In addition, data for impactites from Clearwater East and the K-Pg boundary (Petriccio, Italy) are shown together with data for low-Ir iron meteorites. 4 = McDonald (2002), 5 = Evans et al. (1993), 6 = Petaev and Jacobsen (2004).

samples analyzed, including Layer 2 and Layer 3. Slightly elevated abundances of some volatile elements in some of the layers would be supportive of a volcanic source.

Abundances of selected highly siderophile elements (Re, Os, Ir, Pt, Ru and Pd) and Re-Os isotope ratios from seven sediment samples from the Grotta dei Baffoni Cave, including tephra Layer 3 and samples from above and below this horizon, were measured. Iridium concentrations in the samples range from 0.015 to 0.051 ppb, within the typical range for upper continental crust (UCC), which has an average Ir content of around 0.022 ppb (Peucker-Ehrenbrink and Jahn, 2001). The samples show a dichotomy in Os concentrations and can be divided in low-Os samples (layers 1 and 2, as well as 6 and 7; ranging from 0.034 to 0.089 ppb) that are within the range for UCC (0.031 ppb; Peucker-Ehrenbrink and Jahn, 2001) and high-Os samples (layer 4 and 5, ranging from 3.20 to 4.36 ppb). Tephra Layer 3 has an Os concentration of ~0.21 ppb. Rhenium concentrations are quite homogeneous throughout the samples and mostly range from ~0.10 to ~0.17 ppb, slightly lower compared to UCC (~0.2 ppb; Peucker-Ehrenbrink and Jahn, 2001). Platinum, Ru, and Pd concentrations range from ~0.6 to ~2.1 ppb, from ~0.08 to ~0.17 ppb and from ~1.0 to ~5.5 ppb, respectively (compared to UCC averages of 0.51 ppb, 0.21 ppb and 0.52 ppb, respectively; Peucker-Ehrenbrink and Jahn, 2001).

While none of these concentrations follow the bimodal trend defined by the Os concentrations, the $^{187}Os/^{188}Os$ ratios do: layers 3 and 5 show the least radiogenic $^{187}Os/^{188}Os$ ratios (between ~0.42 and ~ 0.46)

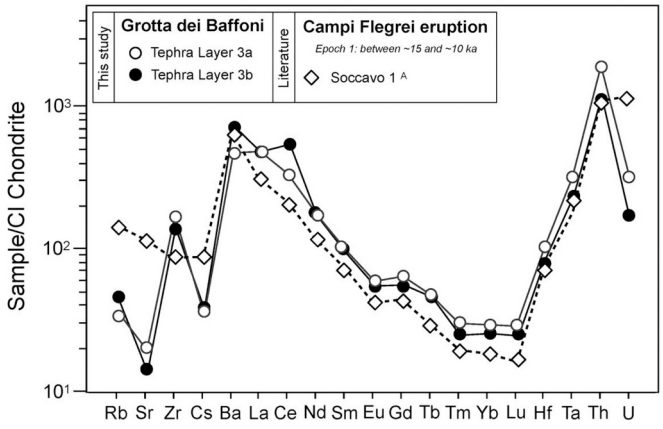

Fig. 4. Chondrite-normalized trace element patterns for two samples from Grotta dei Baffoni tephra Layer 3 and from the Soccavo 1 eruption from Campi Flegrei as representative of Epoch 1 eruptions dated between ~15 and 10.6 ka. Chondrite values from Anders and Grevesse (1989). A = Data from Smith et al. (2011).

Table 3
Platinum group elements (PGE) and Os isotope data for the sedimentary succession of the Grotta dei Baffoni Cave.

Layer (n.) and site	Re (ppb)	(± 2s)	Os (ppb)	(± 2s)	Ir (ppb)	(± 2s)	Pt (ppb)	(± 2s)	Ru (ppb)	(± 2s)	Pd (ppb)	(± 2s)	$^{187}Os/^{188}Os$ (ratio)	(± 2s)	$^{187}Re/^{188}Os$ (ratio)	(± 2s)
(1) GDB/21-PIT2	0.021	0.002	0.034	0.001	0.022	0.003	0.575	0.090	0.096	0.004	3.918	0.161	1.0011	0.0026	3.301	0.505
(2) GDB/21-PIT2	0.159	0.005	0.089	0.001	0.051	0.003	2.128	0.115	0.173	0.008	1.170	0.042	0.9580	0.0024	9.443	0.412
(3) GDB/21-PIT2	0.145	0.012	0.210	0.004	0.015	0.001	1.570	0.064	0.123	0.003	5.540	0.189	0.4571	0.0084	3.431	0.428
(3) GDB/21-PIT2*	0.174	0.006	0.209	0.005	0.016	0.001	2.106	0.138	0.139	0.005	6.705	0.201	0.3040	0.0047	4.057	0.222
(4) GDB/21-PIT2	0.142	0.008	3.204	0.021	0.037	0.003	1.315	0.099	0.076	0.004	2.894	0.164	0.4209	0.0007	0.219	0.014
(5) GDB/21-PIT2	0.124	0.009	4.360	0.035	0.026	0.001	0.968	0.062	0.080	0.003	2.074	0.075	0.4192	0.0007	0.141	0.011
(6) GDB/21-PIT2	0.144	0.006	0.068	0.001	0.029	0.002	1.777	0.015	0.151	0.005	0.967	0.033	0.9820	0.0098	11.292	0.505
(7) GDB/19-H2	0.098	0.005	0.082	0.001	0.031	0.002	0.833	0.055	0.115	0.003	3.671	0.043	1.0016	0.0096	6.350	0.406

Note: * = replicate; layer (3) is the tephra layer.

compared to the other layers. Layers 1 and 2, as well as 6 and 7, are distinctly more radiogenic, ranging from ~0.96 to ~1.00 (similar to the UCC average of around 1.4; Peucker-Ehrenbrink and Jahn, 2001; see Fig. 3 A-C). Using sample amounts of only ~0.5 g does not rule out nugget effects, produced by inhomogeneous HSE carrier phases and grain distributions, but a replicate analysis of ~0.6 g bulk powder (produced from decigrams of sample material) from tephra Layer 3 shows no, or only minor, within-sample heterogeneities (see Table 2). Although slightly less radiogenic, the replicate analyses of tephra Layer 3 show indistinguishable Os and Ir concentrations. Earlier HSE and *Re*-Os isotope studies on Dryas-related sediments also ruled out significant nugget effects (e.g., Paquay et al., 2009).

Our results for Grotta dei Baffoni follow similar trends as observed by Sun et al. (2020) on bulk samples from the Younger Dryas basal boundary dark layer, and samples from horizons above and below it in Hall's Cave, TX, USA, representing a well-dated and stratigraphically steady sequence. These authors reported UCC-like Ir concentrations throughout the stratigraphic sequence, similar to our study and not supportive for an extraterrestrial admixture. Besides the low Ir contents in Hall's Cave samples (with their only in some cases slightly supra-crustal Pt and Pd abundances) Sun et al. (2020) further substantiated their conclusion of a non-meteoritic origin using mixing calculations based on $^{187}Os/^{188}Os$ ratios and 1/Os abundances between crust components and hypothetical mantle-like Os end-members as represented in worldwide volcanic lava samples. Based on Os concentrations and $^{187}Os/^{188}Os$ ratios, they divided the sediments in Hall's Cave into two groups, with either UCC-like Os concentrations and isotope signatures, or less radiogenic $^{187}Os/^{188}Os$ ratios (ranging from ~0.12 to ~0.42) and corresponding Os concentrations of up to ~4.5 ppb. These authors postulated that the source of the least radiogenic $^{187}Os/^{188}Os$ in Hall's Cave may reflect inheritance of aerosols enriched in Os and associated with airborne volcanic tephra from distant volcanic eruptions. This seems a likely explanation in light of observed enrichments in Os of up to 6 ppb (in conjunction with UCC-like Ir, Pt, and Pd abundances) in, for example, pumice from the Laacher See volcanic event (Green, 2019), showing that such high Os enrichments (as observed for Hall's Cave and Grotta dei Baffoni) can result without the necessity of an extraterrestrial component.

Fig. 3A shows $^{187}Os/^{188}Os$ and 1/Os ratios for the Grotta dei Baffoni samples together with the trends reported in Sun et al. (2020) for Hall's Cave samples. The diagram shows the similarity of the signatures of sediments from the Dryas horizons of both studies. Notably, the least radiogenic samples from Grotta dei Baffoni Cave, including tephra Layer 3, are slightly more radiogenic compared to the lowest values reported for Hall's Cave (~0.41 vs. ~0.12), probably reflecting that HSE-enriched tephra from the most likeliest volcanic source(s) for layer 3 in Grotta dei Baffoni, the Campi Flegrei of southern Italy, have more crustal-like $^{187}Os/^{188}Os$ isotope ratios compared to those volcanics that are needed to explain the mantle-like Os isotope signatures in Hall's Cave sediments. As shown in Fig. 4, extended trace element trends for two samples from tephra layer 3 from Grotta dei Baffoni (see Table 3) closely follow the trend defined by typical volcanics from the Campi Flegrei of similar age (Smith et al., 2011). These Campi Flegrei tephra are phonolites and tephriphonolites according to the classification described in Smith et al. (2011). Notably, the HSE and Re-Os isotope data for the Friedkin sample site (Sun et al., 2021), and various other continental Younger Dryas sample sites analyzed by Paquay et al. (2009), also follow the trend shown in Fig. 3A. These studies also provided evidence against an impact hypothesis for the Dryas event(s).

However, tephra Layer 3 and other horizons from Grotta dei Baffoni Cave, are, besides Os in some of the samples, also enriched in P-PGEs (i.e., Pt and Pd) compared to UCC (Fig. 3B). Peak abundances were observed in Layer 3 for Pd (~5.5 ppb) and Layer 2 for Pt (~2.2 ppb), compared to UCC averages of 0.51 ppb and 0.52 ppb, respectively (Peucker-Ehrenbrink and Jahn, 2001). Such elevated P-PGE concentrations of the horizons in Grotta dei Baffoni need to be explained. Notably,

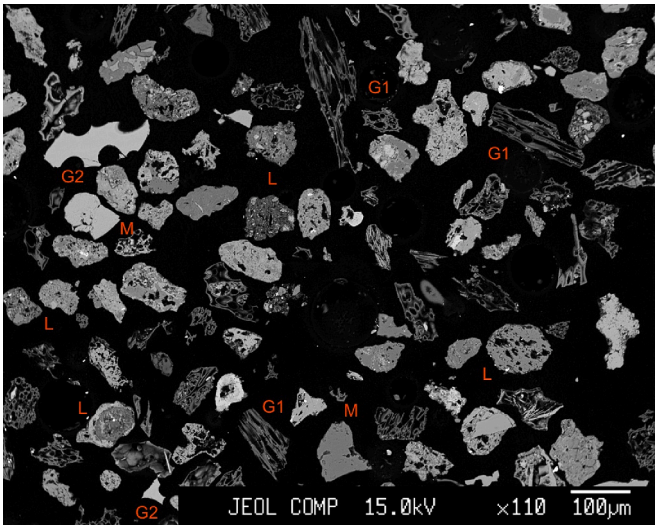

Fig. 5. Back-scattered electron image of the tephra from Layer 3 in the Grotta dei Baffoni cave. Glass shards labelled G1 are the extremely vesicular shards that were not analyzed, and those labelled G2 are the blocky, bubble wall glass shards that formed around circular vesicles. L = lapilli (almost entirely crystallized) and M = mineral grains.

Pt enrichments (in the ppb-range compared to neighboring strata) were reported earlier in Greenland ice cores (possibly linked to the Younger Dryas event) and -at that time- were interpreted to support the claim of a cataclysmic, impact-driven onset of the Younger Dryas (see Petaev et al., 2013). These authors, based on their results, stated that -while inconsistent with chondritic impactors- a low-Ir iron meteorite (similar to Sikhote Alin) could have been the source for the observed Pt signatures in the Greenland ice cores. Although Pt anomalies from other Dryas-related strata were not identified and ever more data argue against the impact hypothesis (see Holliday et al., 2023, and references therein), we (in an attempt to explain the causes for the Pt and Pd abundances in Grotta dei Baffoni Cave) performed simple mixing calculations that show that inconsistent admixtures of Sikhote Alin material of 0.27% for Os and $^{187}Os/^{188}Os$ (cf. Hirata and Masuda, 1992) and admixtures of 0.03% and 0.21% for Pt and Pd would be required to an UCC target in order to generate the measured concentration and $^{187}Os/^{188}Os$ isotope signatures of Grotta dei Baffoni tephra Layer 3, arguing against such a low-Ir iron meteoritic admixture.

Having shown that the Pt and Pd concentrations in our samples cannot self-consistently be explained by an admixture of any known meteoritic components, we can only assume that these enrichments are due to a high Pt and Pd signatures in the volcanic material that might be represented in Layer 3 (either the Campi Flegrei eruption/s at 14.2 ± 0.2 ka or other sources). If such coupled Os and Pt, Pd enrichments are a feature not uncommon in airborne volcanic tephra from major volcanic eruptions, this might also explain some Pt enrichments in the Greenland ice cores investigated earlier (e.g., Petaev et al., 2013; but see also Holliday et al., 2023). In Fig. 3C, we plot the Ir vs. Ir/Pt ratios for the analyzed samples from Grotta dei Baffoni. In line with our conclusions drawn above, the values for tephra Layer 3 (and all other samples analyzed in this study) plot well within the field for volcanic arc samples from worldwide locations, and plot distinctly off the trend defined by typical impactites (containing extraterrestrial components) and meteoritic low-Ir Fe-Ni metal.

3.3. Tephra provenance

Glass shards up to 200 μm in length were identified in the GDB/21-PIT2-L3 sample. Two types of shard morphologies are observed in the sample. Some are extremely vesicular with stretched vesicles and others

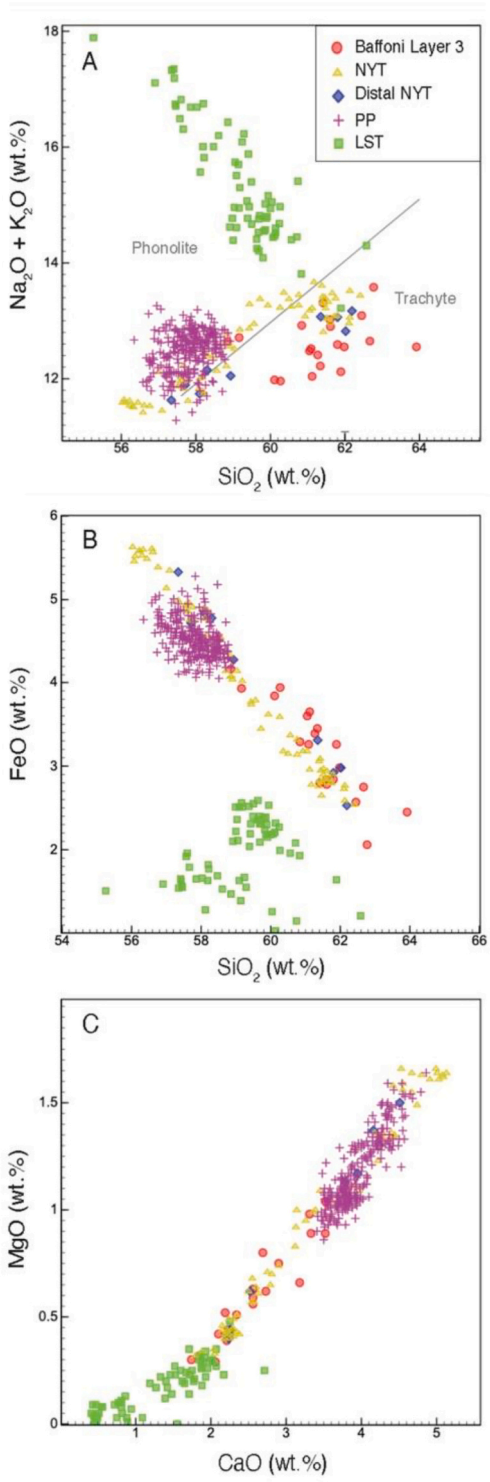

Fig. 6. Glass compositions of tephra in Layer 3 in the Grotta dei Baffoni Cave (red dots; Baffoni Layer 3) plotted against data from the Neapolitan Yellow Tuff (NYT; yellow triangles; data from Tomlinson et al., 2012); distal NYT tephra in Germany (blue triangles; MFM_T1072 in Lane et al., 2015); the 12.037 ± 0.122 cal. BP Pomici Principali (PP) eruption (Ramsey et al., 2015), another large eruption from Campi Felgrei (purple crosses; data from Smith et al., 2011); and the Laacher See Tephra (LST) from the Eifel volcanic field, Germany (green squares; data from Tomlinson et al., 2020). A) Total Alkalis ($Na_2O + K_2O$) versus SiO_2 with the boundary between the Phonolite and Trachyte classification (Le Bas et al., 1986) marked by a grey line; B) SiO_2 versus FeO; and (C) CaO versus MgO. See Table X in Supplementary Material for the raw data. (For interpretation of the references to color in this figure legend, the reader is referred to the web version of this article.)

Table 4
Radiocarbon AMS dating of Layer 2 and Layer 3 from the sedimentary succession of the Grotta dei Baffoni Cave.

Sample name (Layer Nr.) and site	Lab code Nr.	Sample Nr. and fraction	Sample material	C yield (%)	Conv. ^{14}C age (yrs BP ± 1 σ)	Calib. Calendar age (cal BP 2 σ)
(3) GDB/21 Pit-2	DeA-35,471	I/2983/1 L	bulk sediment	0.42	8213 ± 29	9286–9028
(3) GDB/21 Pit-2	*DeA-35,472*	*I/2983/1H*	*bulk sediment*	*0.46*	*8000 ± 30*	*9002–8660*
(2) GDB/21 Pit-2	DeA-35,473	I/2983/2 L	bulk raw sediment	0.45	9513 ± 33	11,072–10,661
(2) GDB/21 Pit-2	*DeA-35,474*	*I/2983/2H*	*bulk raw sediment*	*0.40*	*9793 ± 33*	*11,251–11,184*
(3) GDB/21 Pit-2	DeA-35,475	I/2983/3	charcoal	37.70	12,247 ± 73	14,817–14,701 14,516–13,897
(3) GDB/21 Pit-2	DeA-35,694	I/2983/4	shells	12.40	14,952 ± 72	18,620–18,485 18,319–18,141

Note: BP = Before Present where Present is 1950; *Italic* = control measurement.

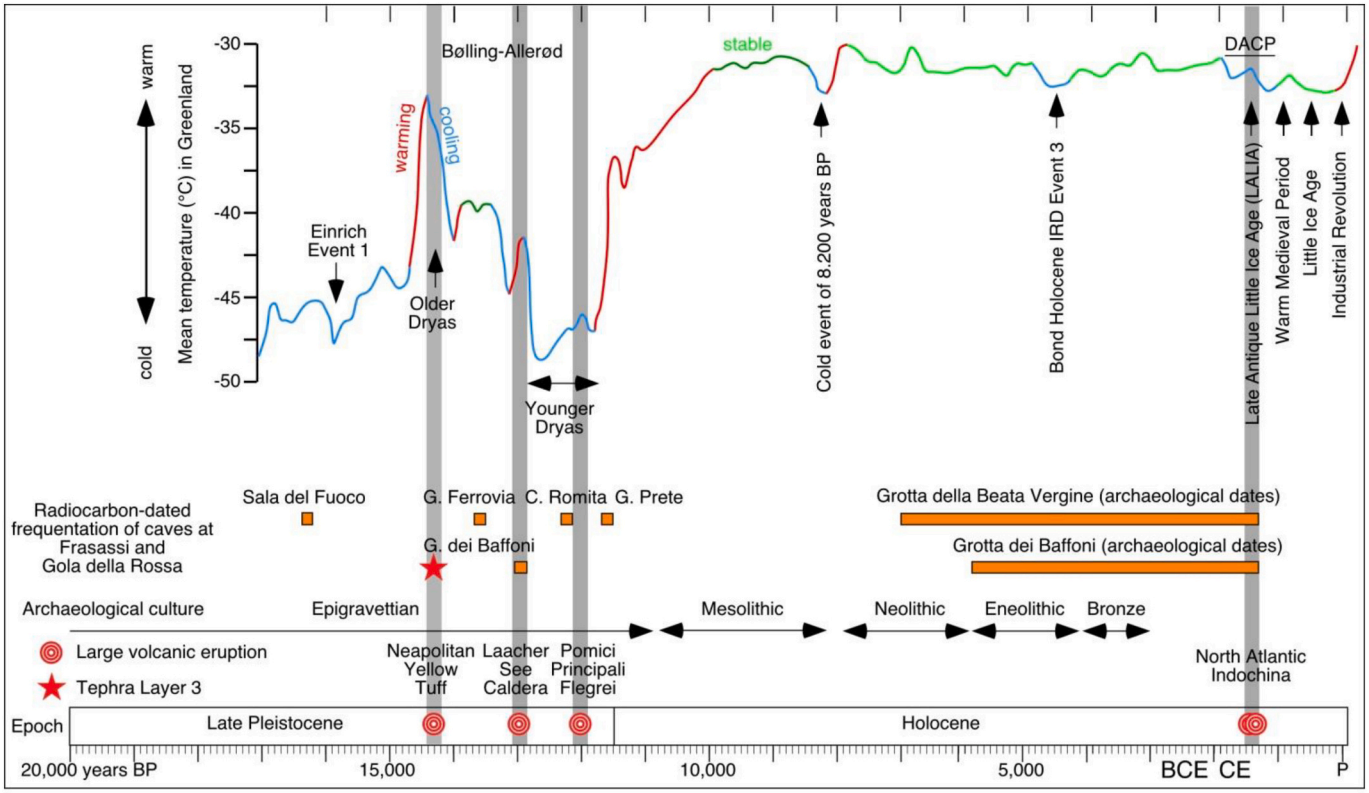

Fig. 7. Synoptic figure of climate changes in the past 17,000 years in relation to major volcanic events and the record of human frequentation in caves of the Frasassi and Gola della Rossa gorges. BP = Before Present; P = Present; BCE = Before Common Era; CE = Common Era. Radiocarbon dating: Sala del Fuoco (Montanari et al., 2020); Grotta della Ferrovia (Alessio et al., 1976); Grotta dei Baffoni (Montanari et al., 2022a); Cava Romita (Guerreschi et al., 2005); Grotta del Prete (Alessio et al., 1970). For the Late Antique Little Ice Age (LALIA), see Montanari et al. (2022b) and references therein; DACP = Dark Ages Cold Period.

are blocky, bubble wall shards that quenched around circular vesicles (see Fig. 5). The blocky shards were analyzed but it was not possible to obtain data on the thin vesicular shards.

The twenty shards from the Grotta dei Baffoni sample that were analyzed are trachytic in composition (Fig. 6 A-C). These shards range in composition, with 58.85 to 63.92 wt% SiO_2, 7.96–9.91 wt% Na_2O, 2.06–4.17 wt% FeO and 1.74–3.52 wt% CaO (Fig. 6 A-C). The composition of these glass shards were compared to those of large eruptions from volcanoes in Europe in the last 15 ka (Tomlinson et al., 2015), including the Laacher See tephra (LST) from the Eifel volcanic region in Germany (Tomlinson et al., 2020). The shards are very similar in composition to eruption deposits from Campi Flegrei volcano in Naples, Campania (Smith et al., 2011) and match the large Neapolitan Yellow Tuff (NYT) eruption (Orsi et al., 1992; Tomlinson et al., 2012) on all elements (Table X in Supplementary Material). The identical glass compositions suggest that the tephra in Layer 3 of Grotta dei Baffoni cave is a distal ash fall from the NYT eruption. The NYT tephra has also been identified as a cryptotephra (concentration of glass shards) in a lake in Germany (>1200 km north of Campi Flegrei; Lane et al., 2015), suggesting that at least part of the eruption plume extended north, which is consistent with the presence of NYT tephra in the Grotta dei Baffoni Cave.

3.4. Radiocarbon geochronology

Two layers (Layer 2 and Layer 3) with 3 different types of materials (charcoal, gastropod shell fragments, and bulk sediment) were dated by radiocarbon analyses (Table 4.). In the case of Layer 2 (GDBB/21 Pit-2) the bulk sediment samples were dated to 11,070–10,660 cal yr BP (L fraction) and 11,250–11,180 cal yr BP (H fraction). While Layer 3 was expected to be stratigraphically older than Layer 2, it yielded younger ages of 9280–9030 cal yr BP (L fraction) and 9000–8660 (H fraction). As shown in Table 4, the dated materials radiocarbon ages are very different from Layer 3. The ages obtained from bulk sediment samples

do not correspond to the stratigraphy suggesting that this material has been reworked. Older than expected ages characterize the gastropod shell fragments ^{14}C dates (14,952 ± 72 ^{14}C yr BP). The charcoal from tephra Layer 3, with an age of ~14.4 ka, is consistent, within radiometric uncertainty, with the age of the Neapolitan Yellow Tuff, but it is definitively older that the age of ~12.9 ka for the Younger Dryas and the age of ~12.85 ka for the charcoal in Layer 2 as determined by Montanari et al. (2022a). The age of ~18.3 ka for the shell fragments in Layer 3 is much older than the charcoal from the same layer because those terrestrial gastropods were washed out from the soil of the atrial area of the cave and re-deposited in the water pool at the far end of the cave, as suggested by Montanari et al. (2022a).

Recently, Bard et al. (2023), on the basis of a detailed ^{14}C geochronological analysis of some 400 subfossil trees preserved in Upper Pleistocene fluvial deposits in the Southern France Alps, discovered a spike of ^{14}C at 14.300 cal yr BP and a following century-long event between 14.0 and 13.9 ka. An exact chronological correspondence with a ^{10}Be anomaly recorded in ice cores allowed Bard and co-authors to propose the 14.3 ka event as a solar energetic particle event, most probably a common Maunder-type solar minimum linked to the modulation of galactic cosmic particles by the heliomagnetic field. They also speculated about the synchronicity and the possible causes of the 14 ka event with the brief cold phase of the Older Dryas, which separates the Bølling and Allerød warm phases of the Late Glacial period. Nevertheless, Bard et al. (2023) concluded that "The causes of these two, millennium-long, events [Older Dryas and Younger Dryas] are the subject of a large amount of literature mainly dealing with the impact of glacial meltwater from the North American and North European ice sheets, which disappeared during the last deglaciation. By contrast, the exact causes of the Older Dryas are largely unknown and unexplored". In other words, the "… solar minimum could have contributed to the cooling but the overall amplitude of the total solar irradiance change expected from such a Maunder-type solar minimum is clearly insufficient" (Bard et al., 2023), as to say that the anomalies observed during the Older Dryas are just consequences of a climatic change and not solar proxies that can be used to identify its cause.

4. Conclusions

Our study of the upper Pleistocene sedimentary succession in the Grotta dei Baffoni Cave revealed that an 1–2 cm-thick tephra Layer 3 contained therein was derived from the explosion of the Campi Flegrei caldera, ~400 km SE of Grotta dei Baffoni Cave, the second largest eruption recorded in this area in the past 15 kyr, with a magma outpour of 0.5 km^3 (Smith et al., 2011), which generated the giant Neapolitan Yellow Tuff some 14.1 ± 1.4 kyr ago. Therefore, we interpret the tephra of Layer 3 as an air fall volcanic ash, which engulfed the cave environment to eventually settle in a water pool at the far end of the cave, some 40 m from the wide, south-facing entrance. Trace element and osmium isotope analysis of each of the 7 layers of this ~80-cm-thick sedimentary deposit did not reveal any evidence for an extraterrestrial signature that could be related to a meteorite impact, which some researchers have advocated as the cause of the sudden and drastic Younger Dryas freezing event of ~12.9 kyr ago (e.g., Moore et al., 2019, 2020, and references therein, but see also Jaret and Harris, 2021, and, especially, Holliday et al., 2023). However, our geochemical investigation did not reveal any evidence for deposits from the explosion of the Laacher See caldera, which occurred ~13.0 kyr ago in central Germany, some 900 km NNW of Grotta dei Baffoni Cave. Nevertheless, Sun et al. (2020) did find geochemical traces of a volcanic event, possibly related to the Laacher See, in the Texan Hall's Cave in a layer dated at around 13.0 ka, proposing that the eruption of this volcano may have triggered the Younger Dryas climatic event. Similar results were obtained from another site by Sun et al. (2021). On the other hand the eruption that generated the Neapolitan Yellow Tuff, to which our tephra layer in the Grotta dei Baffoni Cave is undoubtedly related, is coincidental with the Older Dryas cooling event, a much milder climatic event preceding the Younger Dryas by 1300 years (see synoptic Fig. 7).

It is possible that the exceptionally large volcanic explosion of the Campi Flegrei caldera near Naples (i.e., the Neapolitan Yellow Tuff), which produced the distal tephra Layer 3 in the Grotta dei Baffoni Cave, may have been the trigger of the brief Older Dryas cooling event. As for the more drastic and long lasting Younger Dryas event of 12.9 kyr ago, the present study excludes an extraterrestrial impact as a cause, and concords with Sun et al. (2020) and Reinig et al. (2021) that the trigger may have been an exceptional volcanic explosion, namely the Laacher See event in central Germany (see synoptic Fig. 7).

CRediT authorship contribution statement

Alessandro Montanari: Writing – review & editing, Writing – original draft, Methodology, Investigation, Conceptualization. **Christian Koeberl:** Writing – review & editing, Writing – original draft, Resources, Project administration, Methodology, Investigation, Formal analysis, Data curation, Conceptualization. **Toni Schulz:** Writing – review & editing, Writing – original draft, Methodology, Investigation. **Victoria C. Smith:** Writing – review & editing, Methodology, Investigation, Data curation. **Mihály Molnár:** Writing – review & editing, Methodology, Investigation. **Katalin Tóth-Hubay:** Writing – review & editing, Methodology, Investigation.

Declaration of competing interest

The authors declare that they have no known competing financial interests or personal relationships that could have appeared to influence the work reported in this paper.

Data availability

Data will be made available on request.

Acknowledgements

This research was supported by the non-profit Association "Le Montagne di San Francesco" (www.coldigioco.org). We would like to thank Maurizio Mainiero for helping sampling the section in PIT-2 in the Grotta dei Baffoni Cave. Thanks to D. Mader (Univ. Vienna) for help with the INAA work. We would like to thank Jörg Elis Hoffmann from the Freie Universität Berlin (FUB) for assistance during ICP-MS measurements. We are grateful to the editor, S. Calvari, and two anonymous reviewers for helpful comments.

Appendix A. Supplementary data

Supplementary data to this article can be found online at https://doi.org/10.1016/j.jvolgeores.2024.108067.

References

Alessio, M., Bella, F., Improta, S., Belluomini, G., Cortesi, C., Turi, B., 1970. University of Rome carbon 14 dates VIII. Radiocarbon 12, 599–616.
Alessio, M., Bella, F., Improta, S., Belluomini, G., Calderoni, G., Cortesi, C., Turi, B., 1976. University of Rome carbon-14 dates XIV. Radiocarbon 18, 321–349.
Anders, E., Grevesse, N., 1989. Abundances of the elements: Meteoritic and solar. Geochim. Cosmochim. Acta 53, 197–214.
Bard, E., Miramont, C., Capano, M., Guibal, F., Marschal, C., Rostek, F., Tuna, T., Fagault, Y., Heaton, T.J., 2023. A radiocarbon spike at 14300 cal yr BP in subfossil trees provides the impulse response function of the global carbon cycle during the Late Glacial. Philos. Trans. A 381, 1–22.
Cohen, A., Waters, F., 1996. Separation of osmium from geological materials by solvent extraction for analysis by thermal ionisation mass spectrometry. Anal. Chim. Acta 332, 269–275.
Evans, N.J., Gregoire, D.C., Grieve, R.A.F., Goodfellow, W.D., Veizer, J., 1993. Use of platinum-group elements for impactor identification: terrestrial impact craters and Cretaceous-Tertiary boundary. Geochim. Cosmochim. Acta 57, 3737–3748.

Firestone, R.B., West, A., Kennett, J.P., Becker, L., Bunch, T.E., Revay, Z.S., et al., 2007. Evidence for an extraterrestrial impact 12,900 years ago that contributed to the megafaunal extinctions and the Younger Dryas cooling. Proc. Natl. Acad. Sci. U.S.A. 104, 16016–16021.

Green, C., 2019. Investigating the Origin of a Greenland Ice Core Geochemical Anomaly Near the Bølling-Allerød/Younger Dryas Boundary. Master's Thesis. Durham University, 133 pp.

Guerreschi, A., Silvestrini, M., Peresani, M., Esu, D., Gallini, V., Magnatti, M., Muratori, S., 2005. I depositi epigravettiani del sito 1 di Cava Romita: cronologia, faune, industria litica. In: Preistoria e Protostoria delle Marche, Atti della XXXVIII Riunione Scientifica dell'Istituto Italiano di Preistoria e Protostoria, Portonovo, Abbazia di Fiastra, 1-5 ottobre 2003, Firenze I, pp. 117–130.

Hatté, C., Hodgins, G., Holliday, V., Jull, A.J.T., 2010. Dating human occupation on diatomsphytolith rich sediment: study case Mustang Spring and Lubbock Lake, Texas, USA. Radiocarbon 52 (1), 13–24.

Hirata, T., Masuda, A., 1992. Rhenium and osmium systematics on iron and stony iron meteorites. Meteoritics 27, 568–575. https://doi.org/10.1111/j.1945-5100.1992.tb01078.x.

Holliday, V.T., Daulton, T.L., Bartlein, P.J., Boslough, M.B., Breslawski, R.P., Fisher, A.E., Jorgeson, I.A., Scott, A.C., Koeberl, C., Marlon, J., Severinghaus, J., Petaev, M.I., Claeys, P., 2023. Comprehensive refutation of the Younger Dryas Impact Hypothesis (YDIH). Earth Sci. Rev. 247 https://doi.org/10.1016/j.earscirev.2023.104502. #104502.

Jaret, S.J., Harris, R.S., 2021. No mineralogical or geochemical evidence of impact at Tall el-Hammam, a Middle Bronze Age city in the Jordan Valley near the Dead Sea. Sci. Rep. 12, #5189.

Jochum, K.P., Stoll, B., Herwig, K., Willbold, M., Hofmann, A.W., Amini, M., Aarburg, S., Abouchami, W., Hellebrand, E., Mocek, B., Raczek, I., et al., 2006. MPI-DING reference glasses for in situ microanalysis: New reference values for element concentrations and isotope ratios. Geochem. Geophys. Geosyst. 7, Q02008.

Jull, A.J.T., Burr, G.S., 2006. Accelerator mass spectrometry: is the future bigger or smaller? Earth Planet. Sci. Lett. 243, 305–325.

Koeberl, C., Claeys, P., Hecht, L., McDonald, I., 2012. Geochemistry of impactites. Elements 8, 37–42.

Lane, C.S., Brauer, A., Martín-Puertas, C., Blockley, S.P.E., Smith, V.C., Tomlinson, E.L., 2015. The Late Quaternary tephrostratigraphy of annually laminated sediments from Meerfelder Maar, Germany. Quat. Sci. Rev. 122, 192–206. https://doi.org/10.1016/j.quascirev.2015.05.025.

Le Bas, M., Maitre, R.L., Streckeisen, A., Zanettin, B., IUGS Subcommission on the Systematics of Igneous Rocks, 1986. A chemical classification of volcanic rocks based on the total alkali-silica diagram. J. Petrol. 27 (3), 745–750.

Luguet, A., Nowell, G.M., Pearson, D.G., 2008. $^{184}Os/^{188}Os$ and $^{186}Os/^{188}Os$ measurements by Negative Thermal Ionisation Mass Spectrometry (N-TIMS): effects of interfering element and mass fractionation corrections on data accuracy and precision. Chem. Geol. 248, 342–362.

Luguet, A., Behrens, M., Pearson, D.G., König, S., Herwartz, D., 2015. Significance of the whole rock Re–Os ages in cryptically and modally metasomatised cratonic peridotites: constraints from HSE–Se–Te systematics. Geochim. Cosmochim. Acta 164, 441–463.

Mader, D., Koeberl, C., 2009. Using instrumental neutron activation analysis for geochemical analyses of terrestrial impact structures: current analytical procedures at the University of Vienna geochemistry activation analysis laboratory. Appl. Radiat. Isot. 67, 2100–2103.

McDonald, I., 2002. Clearwater East impact structure: a re-interpretation of the projectile type using new platinum-group element data from meteorites. Meteorit. Planet. Sci. 37, 459–464.

Molnár, M., Janovics, R., Major, I., Orsovszki, J., Gönczi, R., Veres, M., Leonard, A.G., Castle, S.M., Lange, T.E., Wacker, L., Hajdas, I., Jull, A.J.T., 2013. Status report of the new AMS C-14 preparation lab of the Hertelendi Laboratory of Environmental Studies. Debrecen. Hungary. Radiocarb. 55 (2-3), 665–676.

Montanari, A., Adamek, A., Curatolo, A., Ferretti, M.P., Mainiero, M., Mariani, S., McGee, D., Pignocchi, G., Recanatini, S., 2020. An Epigravettian hypogeal site in the Grotta del Fiume Cave at Frasassi (northeastern Apennines, Italy): environmental and geochronologic assessments. Int. J. Speleol. 49 (2), 87–105.

Montanari, A., Ferretti, M.P., Mainiero, M., McGee, D., Pignocchi, G., Recanatini, S., Zorzin, R., 2022a. Revisiting the archaeological site of Grotta dei Baffoni Cave (Frasassi Gorge, Italy): integrated stratigraphy, archaeometry, and geochronology of upper Pleistocene–Holocene cave sediments. In: Koeberl, C., Claeys, P., Montanari, A. (Eds.), From the Guajira Desert to the Apennines, and from Mediterranean Microplates to the Mexican Killer Asteroid: Honoring the Career of Walter Alvarez, Geological Society of America Special Paper, vol. 557, pp. 583–600.

Montanari, A., Mainiero, M., Farabollini, P., Pignocchi, G., 2022b. Sedimentological and archaeological evidence for a Late Antique Little Ice Age climate event (536–660 CE) as recorded in a fluvial strath terrace of the Esino River (Marche Region, Italy). In: Koeberl, C., Claeys, P., Montanari, A. (Eds.), From the Guajira Desert to the Apennines, and from Mediterranean Microplates to the Mexican Killer Asteroid: Honoring the Career of Walter Alvarez, Geological Society of America Special Paper, vol. 557, pp. 571–582.

Moore, C.R., Brooks, M.J., Goodyear, A.C., Ferguson, T.A., Perrotti, A.G., Mitra, S., Listecki, A.M., et al., 2019. Sediment cores from White Pond, South Carolina, contain a platinum anomaly, pyrogenic carbon peak, and coprophilous spore decline at 12.8 ka. Sci. Rep. 9, 1–11. #15121.

Moore, A.M.T., Kennett, J.P., Napier, W.M., Bunch, T.E., Weaver, J.C., Le Compte, M., et al., 2020. Evidence of cosmic impact at Abu Hureyra, Syria at the Younger Dryas onset (~12.8 ka): high-temperature melting at >2200 °C. Sci. Rep. 10, 1–22. #4185.

Norris, S.L., Garcia-Castellanos, D., Jansen, J.D., Carling, P.A., Margold, M., Woywitka, R.J., Froese, D.G., 2021. Catastrophic drainage from the northwestern outlet of glacial Lake Agassiz during the Younger Dryas. Geophys. Res. Lett. 48 e2021GL093919.

Orsi, G., D'Antonio, M., Vita, S., Gallo, G., 1992. The Neapolitan Yellow Tuff, a large-magnitude trachytic phreatoplinian eruption: eruptive dynamics, magma withdrawal and caldera collapse. J. Volcanol. Geotherm. Res. 53, 275–287. https://doi.org/10.1016/0377-0273(92)90086-s.

Paquay, F.S., Goderis, S., Ravizza, G., Vanhaeck, F., Boyd, M., Surovell, T.A., Holliday, V.T., Haynes Jr., C.V., Claeys, P., 2009. Absence of geochemical evidence for an impact event at the Bølling-Allerød/Younger Dryas transition. Proc. Natl. Acad. Sci. U.S. A. 106, 21505–21510.

Pearson, D.G., Woodland, S.J., 2000. Solvent extraction/anion exchange separation and determination of PGEs (Os, Ir, Pt, Pd, Ru) and Re-Os isotopes in geological samples by isotope dilution ICP-MS. Chem. Geol. 165, 87–107.

Petaev, M.I., Jacobsen, S.B., 2004. Differentiation of metal-rich meteoritic parent bodies: I. Measurements of PGEs, Re, Mo, W, and Au in meteoritic Fe-Ni metal. Meteorit. Planet. Sci. 39, 1685–1697.

Petaev, M.I., Huang, S., Jacobsen, S.B., 2013. Large Pt anomaly in the Greenland ice core points to a cataclysm at the onset of Younger Dryas. Proc. Natl. Acad. Sci. U.S.A. 110, 12917–12920.

Peucker-Ehrenbrink, B., Jahn, B.-M., 2001. Rhenium-osmium isotope systematics and platinum group element concentrations: loess and the upper continental crust. Geochem. Geophys. Geosyst. (G3) 2 (22), 2001GC000172.

Pignocchi, G., Montanari, A., 2016. La Grotta della Beata Vergine di Frasassi (Genga – AN): vecchi e nuovi dati geo-archeologici. Riv. Sci. Preist. 68, 143–180.

Pinter, N., Scott, A.C., Daulton, T.L., Podoll, A., Koeberl, C., Anderson, R.C., Ishman, S.E., 2011. The Younger Dryas impact hypothesis: a requiem. Earth-Sci. Rev. 106, 247–264.

Ramsey, C.B., Albert, P.G., Blockley, S.P.E., Hardiman, M., Housley, R.A., Lane, Christine S., Lee, C.S., Matthews, I.P., Smith, V.C., Lowe, J.J., 2015. Improved age estimates for key Late Quaternary European tephra horizons in the RESET lattice. Quat. Sci. Rev. 118, 18–32.

Rehkämper, M., Halliday, A.N., 1997. Development and application of new ion-exchange techniques for the separation of the platinum group and other siderophile elements from geological samples. Talanta 44 (4), 663–672.

Reimer, P.J., et al., 2020. The IntCal20 northern hemisphere radiocarbon age calibration curve (0-55 cal kBP). Radiocarbon 62, 725–757.

Reinig, F., Wacker, L., Jöris, O., Oppenheimer, C., Guidobaldi, G., Nievergelt, D., Adolphi, F., et al., 2021. Precise date for the Laacher See eruption synchronizes the Younger Dryas. Nature 595, 66–69.

Schulz, T., Koeberl, C., Luguet, A., Van Acken, D., Mohr-Westheide, T., Ozdemir, S., Reimold, W.U., 2017. New constraints on the Paleoarchean meteorite bombardment of the Earth – geochemistry and Re-Os isotope signatures of the BARB5 ICDP drill core from the Barberton Greenstone Belt, South Africa. Geochim. Cosmochim. Acta 211, 322–340.

Schulz, T., Luguet, A., Wegner, W., van Acken, D., Koeberl, C., 2016. Target rocks, impact glasses, and melt rocks from the Lonar crater, India: Highly siderophile element systematics and Sr-Nd-Os isotopic signatures. Meteoritics Planet. Sci. 51 (7), 1323–1339. https://doi.org/10.1111/maps.12665.

Smith, V.C., Isaia, R., Pearce, N.J.G., 2011. Tephrostratigraphy and glass compositions of post-15 kyr Campi Flegrei eruptions: implications for eruption history and chronostratigraphic markers. Quat. Sci. Rev. 30, 3638–3660.

Stuiver, M., Polach, H.A., 1977. Discussion: reporting of ^{14}C data. Radiocarbon 19, 355–363.

Sun, N., Brandon, A.D., Forman, S.L., Waters, M.R., Befus, K.S., 2020. Volcanic origin for Younger Dryas geochemical anomalies ca. 12,900 cal B.P. Sci. Adv. 6, 1–10.

Sun, N., Brandon, A.D., Forman, S.L., Waters, M.R., 2021. Geochemical evidence for volcanic signatures in sediments of the Younger Dryas event. Geochim. Cosmochim. Acta 312, 57–74.

Tomlinson, E.L., Arienzo, I., Civetta, L., Wulf, S., Smith, V.C., Hardiman, M., Lane, C.S., Carandente, A., Orsi, G., Rosi, M., Müller, W., Menzies, M.A., 2012. Geochemistry of the Phlegraean Fields (Italy) proximal sources for major Mediterranean tephras: implications for the dispersal of Plinian and coignimbritic components of explosive eruptions. Geochim. Cosmochim. Acta 93, 102–128. https://doi.org/10.1016/j.gca.2012.05.04.

Tomlinson, E.L., Smith, V.C., Albert, P.G., Aydar, E., Civetta, L., Cioni, R., Çubukçu, E., Gertisser, R., Isaia, R., Menzies, M.A., Orsi, G., Rosi, M., Zanchetta, G., 2015. The major and trace element glass compositions of the productive Mediterranean volcanic sources: tools for correlating distal tephra layers in and around Europe. Quat. Sci. Rev. 1–19 https://doi.org/10.1016/j.quascirev.2014.10.028.

Tomlinson, E.L., Smith, V.C., Menzies, M.A., 2020. Chemical zoning and open system processes in the Laacher See magmatic system. Contrib. Mineral. Petrol. 175, 1–18. https://doi.org/10.1007/s00410-020-1657-4.